V International Conference on Particle-based Methods – Fundamentals and Applications
PARTICLES 2017
P. Wriggers, M. Bischoff, E. Oñate, D.R.J. Owen, & T. Zohdi (Eds)

DISCRETE ELEMENT MODELLING OF CONCRETE STRUCTURES UNDER HARD IMPACT

Andria Antoniou[1], Laurent Daudeville[2], Philippe Marin[3], Serguei Potapov[4]
[1]PhD candidate
Université Grenoble Alpes INP/CNRS, 3SR UMR 5521, 38000 Grenoble, France
email: andria.antoniou@3sr-grenoble.fr
URL: https://www.linkedin.com/in/andria-antoniou-713587b7/
[2]Professor
Université Grenoble Alpes INP/CNRS, 3SR UMR 5521, 38000 Grenoble, France
email: laurent.daudeville@univ-grenoble-alpes.fr
URL: http://people.3sr-grenoble.fr/users/ldaudeville/
[3]Associate professor,
Université Grenoble Alpes, CNRS, 3SR UMR 5521, 38000 Grenoble, France
e-mail: philippe_marin@yahoo.fr
URL: https://www.3sr-grenoble.fr/spip.php?article108&lang=fr
[4]Senior research scientist,
IMSIA EDF-CNRS-CEA-ENSTA UMR 9219, 91762 Palaiseau, France
e-mail: serguei.potapov@edf.fr
URL: http://www.imsia.cnrs.fr/spip.php?article105&lang=fr

Key words: DEM, Concrete, Impact, Numerical Modelling

Summary: *The increasing demand for infrastructure security requires accounting the risk of severe loading due to natural or manmade hazards, such as aircraft impacts. This paper presents a Discrete Element Method (DEM) approach implemented in EUROPLEXUS, fast dynamics software, able to predict damage of concrete structures under severe impacts. The proposed DEM model for concrete relies on the original developments of Cundall and Strack for granular materials that was extended to cohesive materials, such as concrete by introducing cohesive interactions in addition to contact ones. In order to validate the DEM approach, the simulation results of three hard impact tests are presented. The tests were performed by CEA Gramat on plain concrete targets with a passive confinement given by a steel jacket surrounding the cylindrical specimen and submitted to the impact of ogive-nosed steel projectiles.*

1 INTRODUCTION

Concrete structures are widely used as shielding barriers to protect sensitive infrastructures. Nowadays, Accidental conditions such as aircraft impacts on nuclear containments, even though, with low probability of occurrence during lifetime of a structure, demand for a designing under extreme loadings. Because of the extreme severity of such a loading, assessment of the protective structures must go far beyond verification of the

resistance to normal operating conditions: it is necessary to investigate the response of the structure until almost its complete failure to assess correctly its ultimate resistance capacity.

While continuous approaches such as the finite element method (FEM) are suitable for the nonlinear analysis of structures before failure, they reach their limits when trying to describe macro cracking and fragmentation mechanisms. The discrete element method (DEM) is a powerful alternative to FEM when advanced damage states and failure of concrete have to be studied. Indeed, DEM allows easily obtaining realistic macro-crack patterns and material fragments due to its discontinuous nature.

In previous paper, a coupled DEM-FEM approach was proposed with soft impact on RC structures [19]. This paper presents a DEM approach able to produce the experimental response of concrete structures under severe loading such as the hard impact due to the turbine of an aircraft engine. A geometric algorithm method based on a tetrahedral finite element mesh is employed for the discrete elements (DE) mesh generation, which uses a disordered assembly of rigid spherical elements of different sizes and masses although the elements do not represent the constituents of concrete. The spheres' interactions are modelled thanks to beam-like elements with a non-linear constitutive behaviour to model damage and compaction (closure of porosity). The strain rate effect is taken into account in tension. The proposed numerical method is validated with the simulation of three hard impact tests conducted by CEA Gramat [18] and the results of two penetration tests and one perforation tests are discussed. All the numerical developments were implemented in EUROPLEXUS [8] fast dynamics software.

2 DISCRETE ELEMENT MODEL

The DEM was originally developed to model granular materials such as sand by Cundall and Strack [4][5]. Afterwards, this method was extended by Hentz to cohesive materials such as concrete, by taking into account the cohesive interaction over the contact interaction [12]. A disordered polydisperse assembly of rigid spherical elements of different sizes and masses, which do not represent the concrete's constituents, is generated by a direct geometric algorithm proposed by Jerier et al. [14] *Figure 1*. The method is based on a special disordering technique of non-overlapping spheres that allows filling a given tetrahedral Finite Element mesh of the modelled specimen. This algorithm was implemented in SherePadder++ [23] free software, which was introduced into the open-source SALOME platform [21]. The DE model aims to reproduce the macroscopic experimental behaviour of concrete. Thus, DE mesh's assembly is required to be isotropic for undamaged concrete, which can be evaluated from the projection of the link's orientation. As has been shown by Potapov et al. [19] a FE mesh with 4 tetrahedra per edge and the ratios maximum over minimum radii $\frac{\text{Rmax}}{\text{Rmin}} = 3$, FE tetrahedron edge over the mean DE diameter $\frac{\text{FE}}{\text{DE}} = 4$ produces a satisfying distribution of interactions.

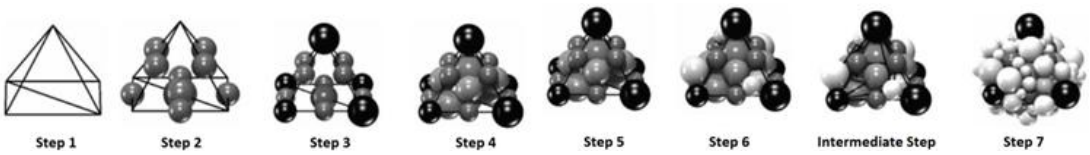

Figure 1 : DE mesh generator technique

2.1 Definition of interactions

An interaction is defined between two spheres a and b of radius R_a and R_b respectively inside an interaction range, which is determined by a interaction coefficient λ *Figure 2*.The two types of links are grouped and treated by the following equation (1), where $D_{a,b}$ is the distance between the centroids of the elements a and b and $\lambda \geq 1$.

$$\lambda\,(R_a + R_b) \geq D_{a,b} \tag{1}$$

A contact interaction is possible, when the distance between two particles is less than or equal to the sum of their radius, thus $\lambda=1$. In contrast, the cohesive interactions exist even when the elements are in certain distance where $\lambda>1$. A cohesive link receives also tensile forces and allows taking into account the effects of the cement matrix in concrete. The cohesive interactions are initialized at the beginning and they exist as long as are not broken whereas the new contact interactions are created throughout the procedure. Contrariwise, a contact link is acting only in compression. The number of links per element with its neighbours varies with the value of λ. The desired number of interactions can be set by adjusting the interaction coefficient. Then, the average number of interactions per discrete element is calculated as the number of links over the number of discrete elements equation (2). An average of 12 links per DE was selected by Rousseau [19].

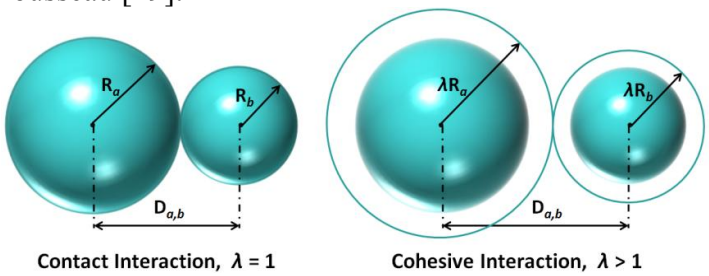

Figure 2: Contact Interaction and Cohesive Interaction

$$\text{average number of interactions per DE} = \frac{\text{number of links}}{\text{number of DE}} \tag{2}$$

2.2 Constitutive behaviour of discrete element concrete model

Unreinforced undamaged concrete is considered to be isotropic, homogeneous elastic and linear, whereas after cracking the behaviour becomes non-linear. Concrete's behaviour is modelled by means of two types of interactions. Contact links can create only contractive forces whereas cohesive links can receive also tensile forces. Two spheres not necessary in contact are related at an equivalent contact point with micro-macro phenomenological sping-like interactions, defined by local normal K_N and tangential K_S stiffnesses [11][19]. A third rolling spring-like interaction, K_R as rolling stiffness, has been implemented by Omar [16] in order to offer rolling resistance to the model and prevent from brittle failure. Moreover, the elastic behaviour of concrete is described by macro-micro relations proposed by Donzé [7], while a modified Mohr-Coulomb criterion is used for non-linear plastic behaviour [12][22].

2.3 Linear elastic constitutive behaviour

The relations for the elastic behaviour were created to describe the local microscopic parameters K_N and K_S from the global macroscopic elasticity coefficients, Young's modulus E, and Poisson's ration ν. The model of concrete in elasticity is originated from Voigt's hypothesis [3] and the best fit hypothesis [15] used for regular assemblies. Those approximations have been modified by Donzé [7] to take into account the disordered assemblies and the size of the interactive elements. Equation (3) shows the micro-macro relations between two elements a and b. $D_{init}^{a,b}$ represents the initial distance between two elements, with radius R_a and R_b and S_{int} is the interaction surface. Young's modulus E, and Poisson's ratio ν are considered the input values of the model whereas α, β and γ parameters need to be identified by mean of linear quasi-static compression and traction tests.

$$\begin{aligned} K_N &= \frac{E\, S_{int}}{D_{init}^{a,b}} \frac{1+\alpha}{\beta(1+\nu)+\gamma\,(1-\alpha\nu)} \quad (a) \\ K_S &= K_N \frac{1-\alpha\nu}{1+\nu} \qquad (b) \end{aligned} \tag{3}$$

Later, a study by Huang [13] has shown the dependence of the elastic macroscopic parameters on the ratio of shear stiffness over normal stiffness K_S/K_N. The expression of Young's Modulus given by Donzé's model [7][6] could be presented dimensionless eliminating its dependence on normal stiffness K_N, by adjusting a value E_0, which derives from the ratio $K_S/K_N = 1$, equation (4). The identification procedure of the linear elastic behaviour parameters α, β and γ is described by Hentz [11]. A compression test with the macroscopic parameters E = 25 GPa and ν = 0.16 performed by Gabet et al. [10] was simulated and the parameters were calibrated, $\alpha = 3.9$, $\beta = 3.75$ and $\gamma = 5$.

$$\frac{E}{E_0} = \frac{\frac{\beta}{\gamma} + \frac{K_S}{K_N}}{\frac{\beta}{\gamma} + 1} \frac{\alpha + 1}{\alpha + \frac{K_S}{K_N}} \tag{4}$$

2.4 Non-linear constitutive behaviour

The non-linear plastic behaviour of concrete, between two elements a and b, in tension is characterized by a local criterion of rupture which found in several studies [12][19][22]. A modified Mohr-Coulomb criterion with sliding function f_1 and a tensile rupture f_2 is used for cohesive links, equation (5). The modified Mohr-Coulomb criterion of cohesive interactions consists from a friction angle Φ_i, a cohesion stress C_0, a local tensile cut off stress T and a softening factor ξ. The softening factor ξ adjusts the tensile stiffness after damage in tension.

$$\begin{aligned} f_1(F_N, F_S) &= |F_S| - \tan(\Phi_i)\, F_N - S_{int} C_o \quad (a.\,\text{Sliding function}) \\ f_2(F_N, F_S) &= -S_{int} T - F_N \qquad\qquad (b.\,\text{Tensile damage}) \end{aligned} \tag{5}$$

The criterion of cohesive interactions equation (5) is separated in the cases below:

$f_2 \leq 0$ and $f_1 \leq 0$, the cohesive link is elastic

$f_2 \leq 0$ and $f_1 = 0$, the shear force follows the sliding function

When the second function, equation (5b) becomes greater than zero the damage of the cohesive link between two elements a and b is initialized because the component of the normal force F_N exceeds the maximum local tensile limit F_{tmax}. Hence, the link passes to the softening phase where the normal stiffness is defined as $\frac{K_N}{\xi}$. This regime is limited to a maximum distance of the two elements D_{el}^{max}. Once the cohesive link is broken and the two spheres come in contact, a new contact interaction is created, which follows a classical Mohr-Coulomb criterion with a contact angle Φ_c, equation (6).

$$f_1(F_N, F_S) = |F_S| - \tan(\Phi_C)\, F_N \quad (a.\,\text{Mohr} - \text{Coulomb}) \tag{6}$$

The criterion of contact interactions is divided in the next cases:

$f_1 \leq 0$, the contact link is opposed to interpenetration

$f_1 = 0$, the shear force follows the sliding function

The compressive non-linear plastic behaviour is governed by the compaction phenomenon, which occurs under high confinement. Once the elastic limit is excited $F_{cel} = \sigma_{cel} S_{int}$, the initialization of microcracks leads to a plastic regime until the plastic limit $F_{cpl} = \sigma_{cpl} S_{int}$, where consolidation take place, after the collapse of porosity and the closure of cracks, with a hardening branch. The stiffness of each branch is defined as the ratio of the initial stiffness of the link K_N over the parameters ξ_1 and ξ_2 respectively.

Figure 3 presents the two models, on the right is plotted the sliding functions, while on the left is illustrated the local link's behaviour. The microscopic parameters of the model need to be identified in order to result the macroscopic parameters, compressive σ_C and tensile σ_T strengths which are obtained from quasi-static tests in tension and compression. The compaction law parameters are defined by means of oedometric and hydrostatic tests obtained thanks to triaxial device that allows performing triaxial compression test on concrete with high confinement pressure. The non-linear behaviour parameters under low pressure were identified as C_0 = 3.5 MPa, T = 3 MPa, ξ = 3, φ_i = 30º and φ_c = 30º by modelling quasi-static tests with macroscopic σ_c = 34 MPa and σ_T = 3.4 MPa, *Figure 4*. For the parameters referred to high pressures σ_{cel} = 0.05GPa, σ_{cpl} = 0.3GPa, ξ_1 =1.5 and ξ_2 =0.3 were employed the Hydrostatic and Oedometric tests, *Figure 5* [10].

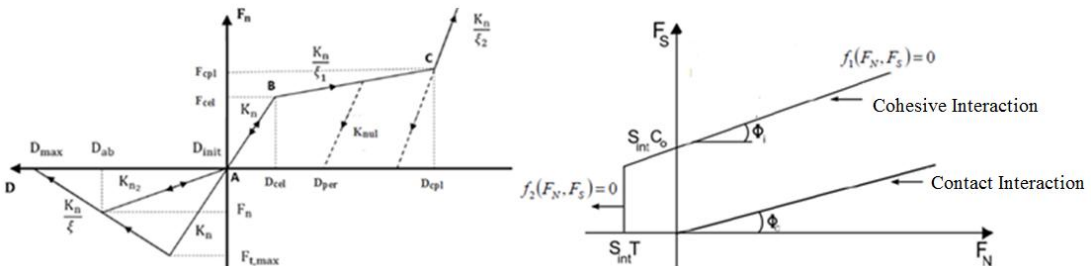

Figure 3: Local criterion of rupture

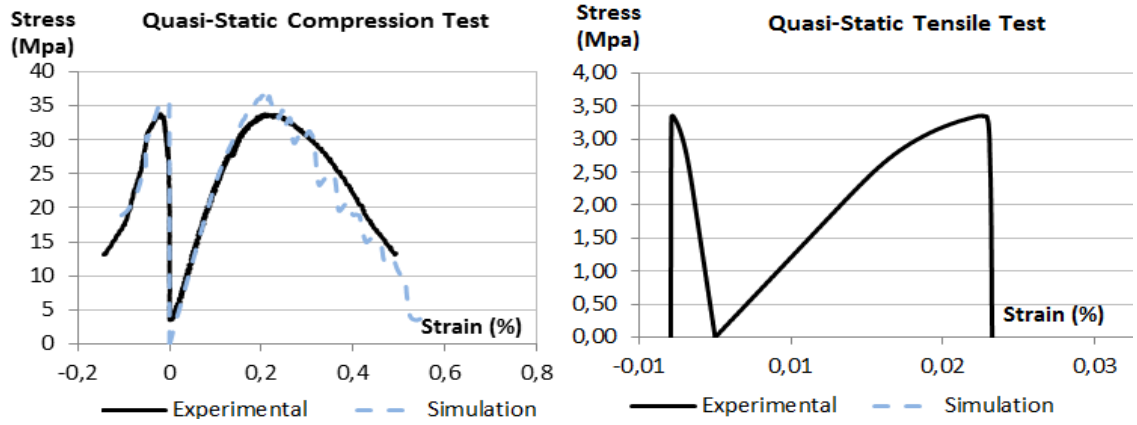

Figure 4: Simulation of quasi-static tests

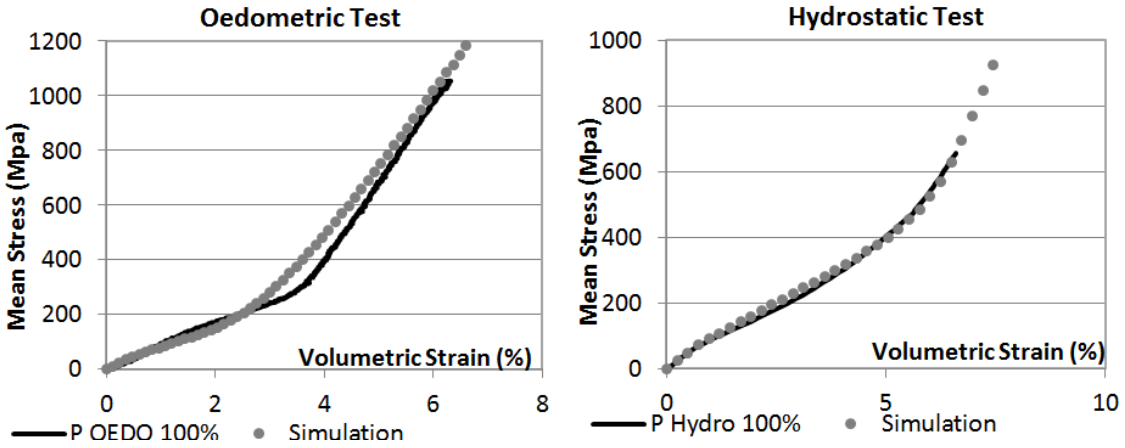

Figure 5: Calibration of under high pressure behaviour parameters, oedometric, hydrostatic tests

2.5 Strain rate dependency

The tensile strength of concrete increases under moderate and high loading rate, as has been observed experimentally. The model has implemented to account for the strain rate sensitivity with the dynamic increase factor (DIF) local equation (7). DIF is defined as the ratio of the dynamic tensile strength over the static tensile strength T_{dyn}/T_{st}. The increase is applied also on the maximum distance limit D_{max}, as can be seen on *Figure 6*. The local parameters $\dot{\varepsilon_{st}}$, $\delta 1$ and $\delta 2$ are calibrated with the help of a Hopkinson bar spalling test [1]. The experimental pullback velocity of the specimen's rear face, is reproduced with the parameters $\dot{\varepsilon_{st}} = 10^{-6}$, $\delta 1 = 0.052$ and $\delta 2 = 0.333$.

$$\mathrm{DIF} = \frac{T_{dyn}}{T_{st}} = \begin{cases} 1 & if\ \dot{\varepsilon} \le \dot{\varepsilon_{st}} \\ \left(\frac{\dot{\varepsilon}}{\dot{\varepsilon_{st}}}\right)^{\delta 1} & if\ \dot{\varepsilon_{st}} < \dot{\varepsilon} \le 1s^{-1} \\ \theta\left(\frac{\dot{\varepsilon}}{\dot{\varepsilon_{st}}}\right)^{\delta 2}, \theta = 10^{(6\delta 1 - 2)} & if\ \dot{\varepsilon} > 1s^{-1} \end{cases} \quad (7)$$

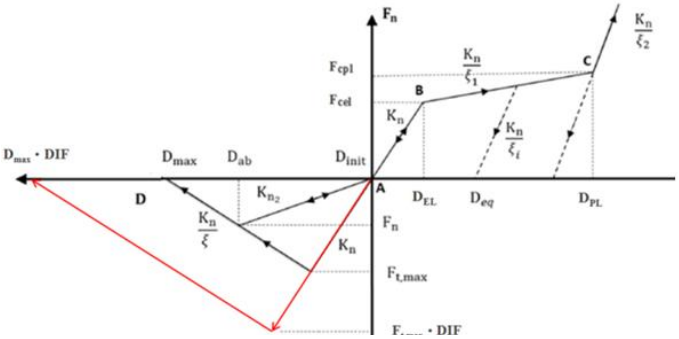

Figure 6: Constitutive model under dynamic loading

3 SIMULATION OF IMPACTS

The reliability of the proposed DEM numerical model is validated with the simulation of high velocity impacts on confined concrete. The numerical results are compared with the experimental data obtained by CEA Gramat.

3.1 Impact experiments

A series of impact tests have performed by CEA-Gramat. Ogive-nosed steel projectiles with a calibre-radius-head (nose radius to diameter ratio) 5.77, a shank diameter of 52.06 mm, a length of 299.43 mm and a mass 2.442 Kg, *Figure 7 (right)* were launched on fully saturated unreinforced cylindrical targets made of ordinary concrete R30A7 confined with a thin steel jacket. R30A7 concrete was widely investigated in previous studies [6]. The impacted specimen diameter is 800 mm, while the thickness is varying with 300 mm for perforation test and 800 mm for penetration test. The confined steel jacket has a thickness of 15 mm and it is anchorage on the concrete target. An accelerometer was embedded into the projectile *Figure 7 (right)* to record the axial deceleration during the experiment. In addition, after the test a topographic laser system was used to measure the crater dimension and the penetration depth. Three tests have been conducted with different striking velocities, one perforation test with 333m/s and two perforation test with higher velocity 347.4 m/s (HV) and lower velocity 227 m/s. "DEIMOS'' gas launcher *Figure 7 (left)* was employed to give the initial impulse on the strikers. *Figure 8* shows the perforation impact test at certain moments *(left)* and the damage mode of the penetration test (HV) *(right)*.

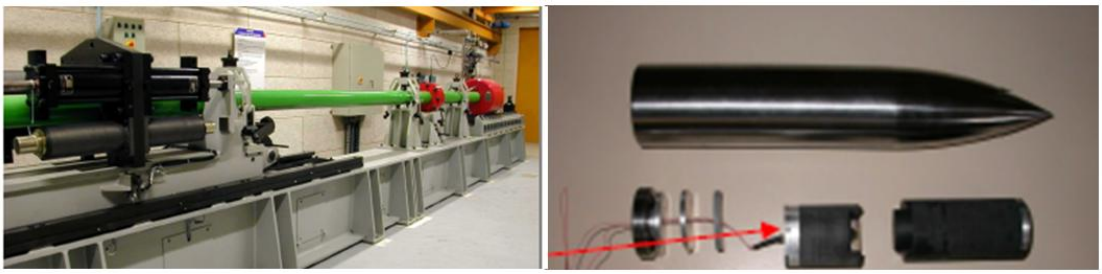

Figure 7: "DEIMOS" gas launcher (left), projectile with its accelerometer

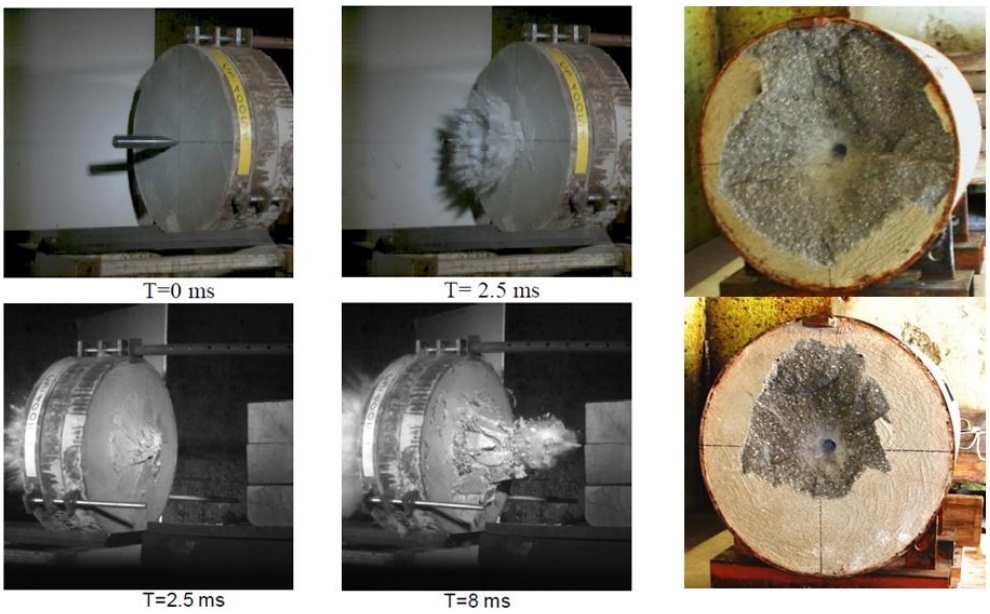

Figure 8: Perforation Impact (left), Penetration Impact (right)

3.2 Modelling of impact experiments

The cylindrical concrete specimen was modelled with DE, while for the steel projectile and the steel confining jacket were used tetrahedral FE, *Figure 9*. All meshes have been generated by using SALOME [21]. The DE concrete mesh was created from an eight tetrahedra FE mesh per short side (of the specimen's geometry) with SherePadder++ [23] direct geometrical algorithm. The eight tetrahedral FE mesh was selected in order to produce spheres with diameters similar to the FE size of the projectile and the steel jacket. The condition of similar sizes between FE and DE should be respected, for proper link creation. **Table 1** illustrates the DE properties of the perforation and penetration test. Furthermore, for the simulations of the three impact experiments 10% of damping was used.

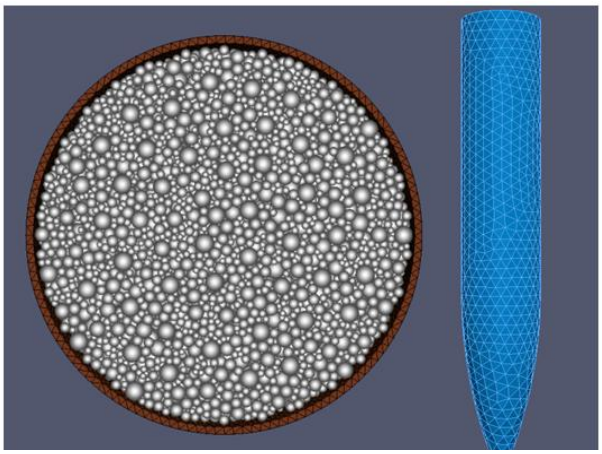

Figure 9: Model of impact test DE concrete with FE confined steel jacket (left), FE steel projectile (right)

Table 1: Properties of perforation and penetration DE meshes

Compactness	DE#	λ	Rmax (cm)	Rmin (cm)	Rmean (cm)
Perforation					
0.6086	141765	1.3986	0.9	0.3	0.471
Penetration					
0.6154	336467	1.402	0.9384	0.3128	0.491

Figure 10 shows the numerical and experimental results for the perforation impact test. On the left side is plotted the axial displacement of the projectile, while on the right side its velocity. Equivalently

Figure 12 presents the results for the penetration impact tests. The crack patter observed experimentally can be found on *Figure 11* for the perforation test and on *Figure 13* for the penetration (HV) test on the right side, whereas on the left side are given the damages obtained from the numerical simulations.

The numerical result has well predicted the experimental results. For the perforation test the results are thoroughly matched. However, a slight difference is observed on the curves of the penetration tests. The damage for both experiments seems to be quite similarly produced by the DE model, with more significant diagonal cracks at the bottom of the perforated specimen than the top. In addition, by comparing *Figure 8 (left)* with *Figure 11 (left)*, it is obvious that the phenomena observed experimentally, such as spalling on the front and scabbing on the rear face, have been successfully generated during the perforation test simulation. Furthermore, a cratering damage mode is following the penetration test, which it has also appeared at numerical results.

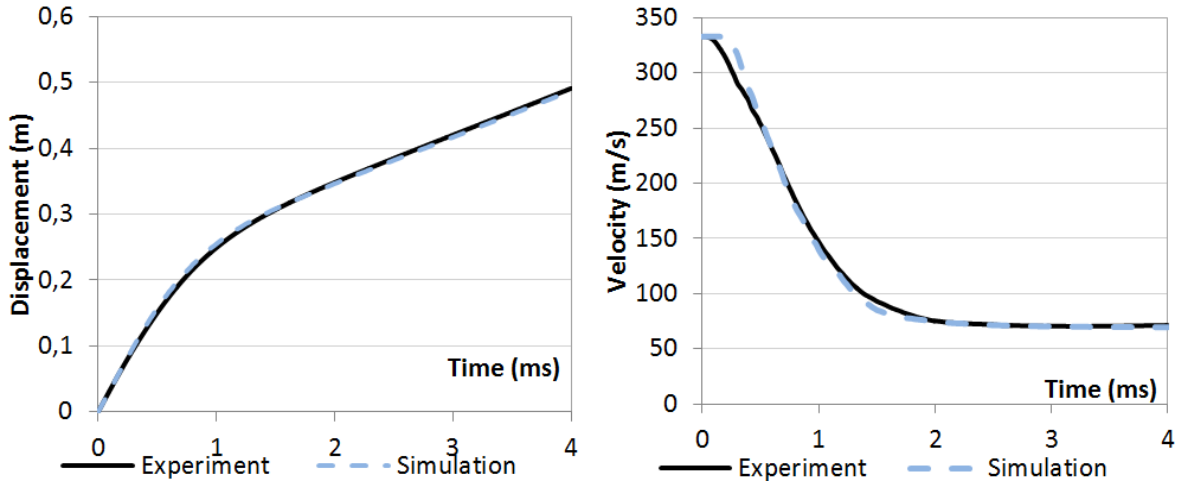

Figure 10: Perforation test, simulation and experiment, projectiles axial displacement (left), velocity (right)

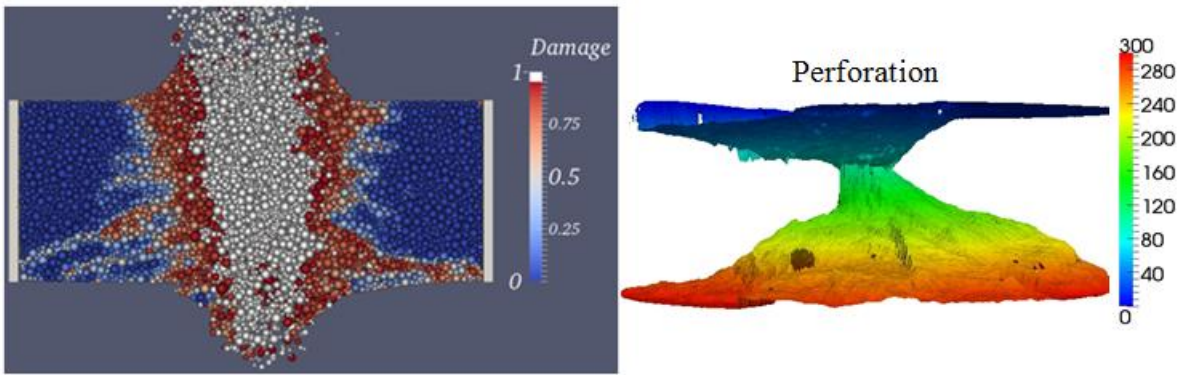

Figure 11: Perforation crack pattern, simulation (left) experiment (right)

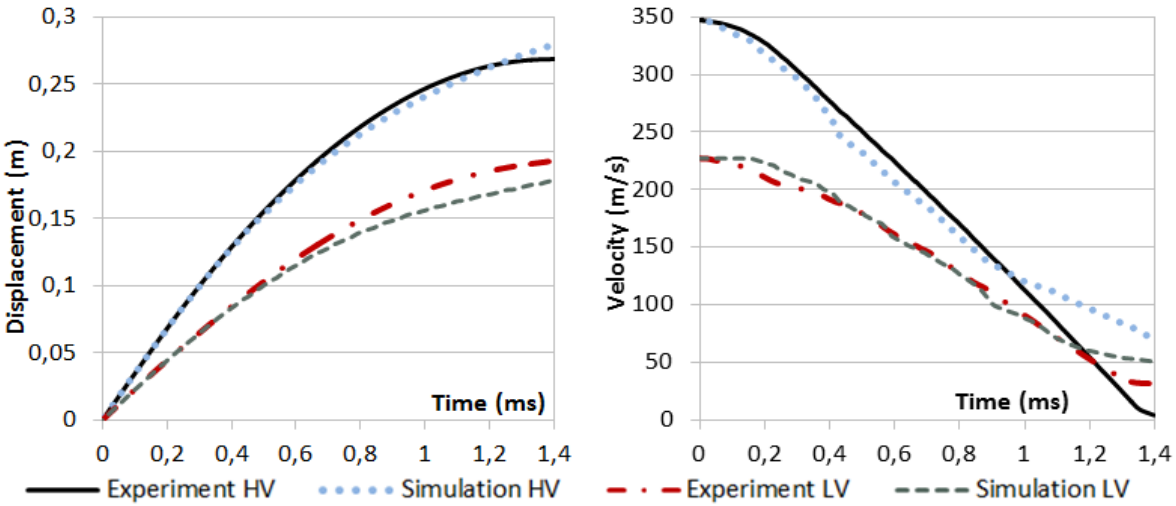

Figure 12: Penetration test, simulation and experiment, projectiles axial displacement (left), velocity (right)

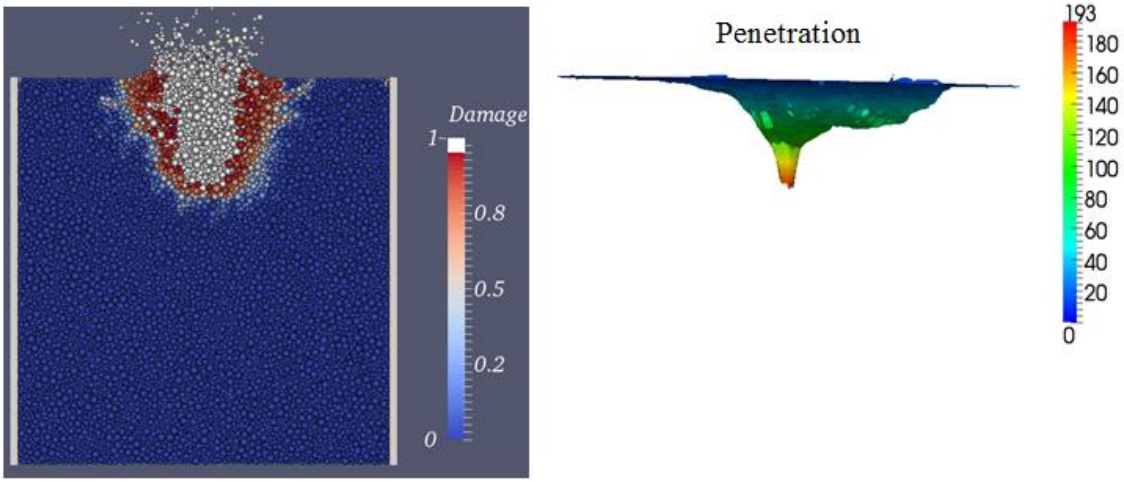

Figure 13: Penetration crack pattern, simulation (left) experiment (right)

4 CONCLUSION

In this paper a numerical method of DEM for concrete has proposed to model structure under severe loadings. The DEM approach has applied to simulate extreme impact experiments on thick confined concrete specimen, which can represent an aircraft strike on a nuclear shielding. Perforation and penetration tests were satisfying reproduce by the numerical results. The crack patterns appeared to be well accordance with the experimental ones. This study gives the motivation to proceed in simulating the response of industrial-size concrete structures.

REFERENCES

[1] Antoniou, A. Contribution to the experimental analysis and numerical modeling of spalling technique into concrete specimens under dynamic tension. Thesis master 2, Université Joseph Fourier, (2014).

[2] Bian, H., Jia, Y., Shao, J. and Pontiroli, C., Numerical study of a concrete target under the penetration of rigid projectile using an elastoplastic damage model, Engineering Structures, Journal Elsevier, p. 525-537 (2016)

[3] Cambou, B., Dubujet, P., Emeriault, F., and Sidoroff, F. (1995). Homogenization for granular materials. European journal of mechanics. A. Solids, 14(2), 255-276.

[4] Cundall, P.A. and Strack, ODL., "Discrete numerical-model for granular assemblies", Geotechnique, 29(1), 47-65 (1979).

[5] Cundall, P.A., Formulation of a three-dimensional distinct element model – Part I, A schele to detect and represent contacts in a system composed of many polyhedral blocks, International Journal of Rock Mechanics and Mining Sciences, Vol. 25, p. 107-116 (1988).

[6] Daudeville L., Malecot Y. 2011. Concrete structures under impact. European Journal of Environmental and Civil Engineering. 15(S1): 101-140.

[7] Donze, F.V., Richefeu, V., Magnier, S-A., Advances in Discrete Element Method Applied to Soil, Rock and Concrete Mechanics, EJGE

[8] EUROPLEXUS, A computer program for analysis of fast transient phenomena involving structures and fluids in interaction, available at http://www-epx.cea.fr

[9] Forquin, P., Sallier, L. and Pontiroli, C., A numerical study on the influence of free water content on the ballistic performance of plain concrete targets, Mechanics of Materials, Journal Elsevier, p. 176-189 (2015)

[10] Gabet, T., Vu, X.H., Malécot, Y. and Daudeville, L., A new experimental technique for the analysis of concrete under high triaxial loading, J.Phys IV. 134: 635-640 (2006).

[11]Hentz S., Daudeville L., Donzé F. “Identification and validation of a discrete element model for concrete, Journal of Engineering Mechanics", vol. 130, n°6, 2004b, p.709-719 (2004).

[12]Hentz, S., Daudeville, L. and Donze, F. V., Discrete element modelling of concrete submitted to dynamic loading at high strain rates. Computers and Structures. 82(29-30): 2509-2524 (2004)

[13]Huang, H., Lecampion, B. and Detournay, E., Discrete element modelling of tool-rock interaction I : rock cutting, International Journal for Numerical and Analytical Methods in Geomechanics 37: p. 1913-1929 (2013)

[14]Jerier J., Imbault D., Donze F. and Doremus P., “A geometric algorithm based on tetrahedral meshes to generate a dense polydisperse sphere packing”, Granular Matter, 11:43–52 (2009a)

[15]Liao, C.-L., Chang, T.-P., Young, D.-H. and Chang, C. S. (1997). Stress-strain relationship for granular materials based on the hypothesis of best fit. Int. j. Solids Structures, 34(31- 32):4087–4100

[16]Omar A., Marin P., Potapov S., Daudeville L. 3D discrete element modeling of concrete: Study of the rolling resistance effects on the macroscopic constitutive behavior., XII International conference on Computetional Plasticity-Fundamentals and Applications, COMPLAS XII Barcelona, p 575-586 (2013)

[17]Omar, A., Marin, P., Forquin, P. and Daudeville, L., Validation of a 3Ddiscrete element model in investigating dynamic tensile behaviour of concrete at high strain rates, 9th International Conference on Structural Dynamics, EURODYN, Porto 2014

[18]Pontiroli C., Erzar B. & Buzaud E. (2014). Concrete behaviour under ballistic impacts: Effects of materials parameters to penetration resistance and modeling with PRM model. Proceedings of Computational Modeling of Concrete and Concrete Structures (EURO-C 2014)

[19]Potapov, S., Masurel, A., Marin, P. and Daudeville, L., Mixed DEM/FEM modelling of advanced damage in reinforced concrete structures, ASCE Journal of Engineering Mechanics, ISSN 0733-9399 (2016)

[20]Rousseau J., Frangin, E., Marin, P., & Daudeville, L. (2008). Damage prediction in the vicinity of an impact on a concrete structure: a combined FEM/DEM approach. *Computers and Concrete*, *5*(4), 343-358.

[21]SALOME, Computer software, http://www.salome-platform.org

[22]Sazamoto, Y., Tsubota, H., Kasai, Y., Kishiba, N., Morikawa, H. (1998). Analytical studies on local damage to reinforced concrete structures under impact loading by discrete element method. Nuclear Engineering and Design, 179:157–177.

[23]SherePadder++, Computer software, https://subversion.assembla.com/svn/spherepadder/

[24]Vu, X. H., Malecot, Y., & Daudeville, L. (2009). Strain measurements on porous concrete samples for triaxial compression and extension tests under very high confinement. *The Journal of Strain Analysis for Engineering Design*, *44*(8), 633-657.